Computer Assisted Mechanics and Engineering Sciences, 11: 247–261, 2004.

Model for the determination of the load carrying capacity of the RC walls

Z. Mišković
Department of Civil Engineering University of Belgrade,
11000 Belgrade, Serbia, Yugoslavia;
mzoran@imk.grf.bg.ac.yu

(Received May 30, 2004)

The paper presents the possibility of the limit stress state approximation of the reinforced concrete wall structures by discontinuous stress fields with variable configuration. Heuristic optimization technique, *simulated annealing,* is applied to determine optimal configuration for approximation of *load carrying capacity* based on *lower bound theorem* of theory of plasticity. Model was tested by comparing with the results of several experimental tested beams, as well as with other numerical models.

Keywords: concrete structures, plastic design, carrying capacity, numerical methods, heuristic optimization, simulated annealing

1. Introduction

Wall structures are structural elements which significantly deviate from the basic assumptions pertaining to beam structures and therefore they must be considered as elements with more complex stress states which could be included in the so called *in-plane stress.* Non-homogeneity of reinforced concrete as composite material makes the theory of elasticity inadequate in comprehension of stress states in these elements, especially in the *state of the limit equilibrium,* which is analyzed in this paper.

Limit states of the reinforced concrete wall structures have been less addressed in research from experimental, theoretical and numerical aspect than limit states of beam and slab structures. In our country, significant and comprehensive research in this area was done by Mirko Aćić [1], as well as several recent researches.

Development of numerical methods, primarily of FEM in 70s and 80s, which was following development of computer technology, resulted in numerous applications of theory of plasticity for analysis of the reinforced concrete structure behaviour. Various models of analysis of the reinforced concrete structures in plane stress state which are implemented in contemporary computer programs could be found in the monography Kostavos and Pavlović [5].

In recent decades, less complex models for analysis load carrying capacity of reinforced wall structures have been developed and improved. Primarily, those models are based on the simple stress fields with practically axially stress state inside particular areas. These stress fields, the so-called *Strut-and-Tie* models, are based on *Ritter's* and *Morsh's* models truss analogy of the inner forces flow in reinforced concrete elements. Also, that models could be found in Schlaich's and Marti's works [14, 6]. A complex stress state which is inherent in nodes of such truss models should be treated, like in [13], as zones in the plane stress state.

Analysis of the *load carrying capacity* of the reinforced concrete elements in plane stress state can also be carried out by the application of *discontinuous stress fields* based on the *lower /static/ bound theorem of theory of plasticity.* Those models are situated between the complex incremental models for FE applications and less complex *Strut-and-Tie* models, which have been widely applied in engineering practice. Examples of those carrying capacity solutions, simple discontinuous stress fields which express stress distribution in the limit state of reinforced concrete structures, can be found in literature, Nielsen [11]. These solutions are based on the constant stress distribution along discontinuity lines, which bound triangular continuous stress areas. Consequence of this assumption is a constant stress state in triangular continuous areas between discontinuity lines. A *computer-based* procedure for designing of such stress fields with application on determining ultimate carrying capacity is developed in R. Hajdin's dissertation [3].

It is well known that quality of the approximation load carrying capacity is conditioned by the configuration of the discontinuous stress field, which expresses stress state in the limit equilibrium. Application of the optimization of discontinuous stress field configuration with the aim to improve approximation of limit stress state of reinforced concrete structures in plane stress state is the subject of this work as well as of the investigation presented in [9].

2. Basic assumptions

Prediction of the load carrying capacity is based on *bound theorems of theory of plasticity* which are established at the beginning of 20th century and strictly defined by Drucker in the 50's. The theorems imply *rigid ideally plastic model* of material behavior, whereby the share of elastic deformation in total deformation is neglected, (1).

$$\varepsilon_{ij} \approx \varepsilon_{ij}^{p}, \quad \varepsilon_{ij}^{e} \approx 0. \tag{1}$$

Following basic postulates of *non-viscous plasticity* (Drucker), the so-called *associated flow law,* are defined, so that the *flow law* is independent of the level of plastic deformations in the case of applied material model ε_{ij}^{p}. The suitable plasticity condition could be shown in the form (2).

$$\Phi(\sigma_{ij}) \leq 0. \tag{2}$$

Bound theorems are defined for the case where all outside loads are proportional to one parameter, *multiplicator of outside load* λ,

$$p_i^{\lambda} = \lambda \cdot p_i^0 \tag{3}$$

whereby the so-called *proportional load* is defined. Also, stress surface conditions must be achieved in the part of the body where external stresses are defined (4),

$$p_i^{\lambda} = \sigma_{ij}\, n_j \qquad \text{on} \qquad S_p \tag{4}$$

as well as local conditions of stress equilibrium with presence of the volume forces (5) and symmetry of the stress tensor (6).

$$\sigma_{ij,j} + f_i = 0 \qquad i, j = 1, 2, \tag{5}$$

$$e_{ij3}\ \sigma_{ij} = 0. \tag{6}$$

The stress distribution which may be assumed in the limit state induced by the plastic collapse, the so called *feasible stress state,* must satisfy the plasticity conditions (2) and stress conditions (4)–(6).

Lower /static/ bound theorem theory of plasticity /LBT/ points out that the load multiplicator –λ^s, which corresponds to the previously defined *feasible stress state,* is always lower then or equal to the real load multiplicator in the state of the limit equilibrium – $\lambda^{\lim}$, (7).

$$\lambda^{s} \geq \lambda^{\lim}. \tag{7}$$

This fact implies that determined limit load is on the safety side, which results in the wide range of applications in solving practical engineering tasks. Another convenient fact is that the theory of plasticity also allows the so-called *discontinuous stress fields* at plastic collapse, which considerably extends the range of feasible *stress states.* It means that a *good enough* approximation of limit stress state may be found out easily.

Discontinuities in the stress field are represented by discontinuity surfaces in the body. Constant stress distribution along elements' thickness implies a possibility to accomplish consideration only in the middle plane of the element. In the middle, plane *discontinuity lines* represent stress field discontinuities, and stress field must be continuous between these lines. The only allowed discontinuity is normal stress discontinuity for the plane with normal vector parallel to the discontinuity line (8), Fig. 1.

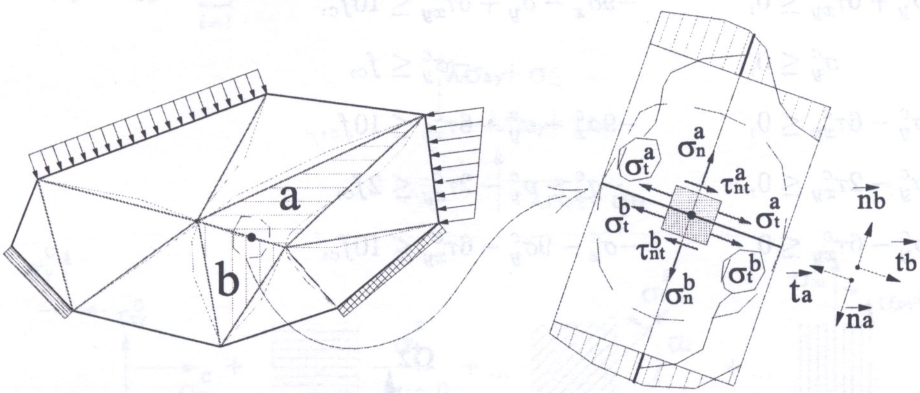

Fig. 1. Allowed stress discontinuity at the limit state of the plane stress

$$\sigma_t^a \neq \sigma_t^b \,. \tag{8}$$

Normal and tangent stresses for the plane with the normal vector orthogonal upon the discontinuity line must be continuous. This reflects continuity of transfer of normal and tangent stresses upon the surface of discontinuity.

$$\sigma_n^a = \sigma_n^b, \qquad \tau_{nt}^a = \tau_{nt}^b \,. \tag{9}$$

Surface conditions, upon the border continuous region rounded by discontinuity lines, expressed by adequate stresses along discontinuity lines must be achieved, as well as equilibrium conditions (5) and local moment equilibrium equations which express symmetry of stress tensors (6). Following continuum mechanics postulates, integration of the equation (5), and application of the *Gauss*' theorem on divergence, equations of global equilibrium of the forces of the whole region will be obtained,

$$\int_S p_i \,\mathrm{d}S + \int_V f_i \,\mathrm{d}V \qquad i = 1,\, 2, \tag{10}$$

i.e. the global moment equilibrium equation

$$\int_V e_{ij\,3}\, \sigma_{ij} \,\mathrm{d}V = 0. \tag{11}$$

These equations must be satisfied for each continuous stress region of the whole field.

In the case of applied *ideally rigid plastic* model of material, limit state of plane stressed concrete is most often represented by the *Modified Mohr-Columb* plasticity condition without tensile strength [10, 11]. It is has also, been applied in this research. This condition is defined by one parameter, pressure strength of concrete, f_c, which is shown in the coordinate system of principal stresses, Fig. 2. Practical reasons of problem solution require linearization of this condition. We assumed linearization with small local violations, as one applied in the research [3], so that generalized condition (2) would be defined by the system (12).

$$
\begin{array}{ll}
\text{zone} - A & \text{zone} - B \\
\sigma_x^c \le 0, & -\sigma_x^c \le f_c, \\
\sigma_x^c + 9\sigma_y^c + 6\tau_{xy}^c \le 0, & -\sigma_x^c - 9\sigma_y^c + 6\tau_{xy}^c \le 10 f_c, \\
\sigma_x^c + \sigma_y^c + 2\tau_{xy}^c \le 0, & -\sigma_x^c - \sigma_y^c + 2\tau_{xy}^c \le 2 f_c, \\
9\sigma_x^c + \sigma_y^c + 6\tau_{xy}^c \le 0, & -9\sigma_x^c - \sigma_y^c + 6\tau_{xy}^c \le 10 f_c, \\
\sigma_y^c \le 0, & -\sigma_y^c \le f_c, \\
\sigma_x^c + 9\sigma_y^c - 6\tau_{xy}^c \le 0, & -9\sigma_x^c - \sigma_y^c - 6\tau_{xy}^c \le 10 f_c, \\
\sigma_x^c + \sigma_y^c - 2\tau_{xy}^c \le 0, & -\sigma_x^c - \sigma_y^c - 2\tau_{xy}^c \le 2 f_c, \\
9\sigma_x^c + \sigma_y^c - 6\tau_{xy}^c \le 0, & -\sigma_x^c - 9\sigma_y^c - 6\tau_{xy}^c \le 10 f_c,
\end{array}
\tag{12}
$$

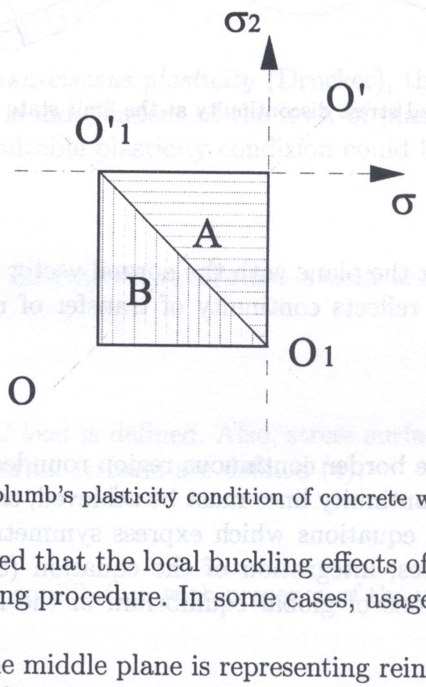

Fig. 2. Modified Mohr–Columb's plasticity condition of concrete without tensile strength

This plasticity condition assumed that the local buckling effects of the compressed reinforcement bars are excluded during the solving procedure. In some cases, usage of the reduced yield strength of the bars may be useful, [9].

The equivalent membrane in the middle plane is representing reinforcement with a possibility of bearing stress upon the direction of reinforcement bars. According to this fact, yield limit parameter of the reinforcing layer, with the bar of cross-sectional area A_i, distance between the bars e_i, yield limit parameter $\bar{f}_Y$ and thickness of the element d, is defined by (13), while plasticity condition becomes (14).

$$f_Y^i = \frac{A_i \bar{f}_Y}{d\, e_i}, \tag{13}$$

$$|\sigma_i^s| \le f_Y^i. \tag{14}$$

Modelling of the common action of concrete and reinforcement in RC as composite material in the limit state problems according the *LBT*, is based on decomposition of the whole stress into separate material stresses, [3, 10]. Here, taking into account the influence of volume forces, the adopted decomposition of stresses is shown in Fig. 3. Applying *load multiplicator* only to the surface load, the relations between the actual stress state and the stresses upon the concrete and layers of reinforcement are expressed by the system (15).

$$\begin{aligned} \lambda\, \sigma_{ax} + \sigma_{fx} &= \sigma_x^c + \sum_{i=1}^{m} \sigma_i^a \left(\cos\alpha_i\right)^2, \\ \lambda\, \sigma_{ay} + \sigma_{fy} &= \sigma_y^c + \sum_{i=1}^{m} \sigma_i^a \left(\sin\alpha_i\right)^2, \\ \lambda\, \tau_{axy} + \tau_{fxy} &= \tau_{xy}^c + \sum_{i=1}^{m} \sigma_i^a \left(\cos\alpha_i \cdot \sin\alpha_i\right). \end{aligned} \tag{15}$$

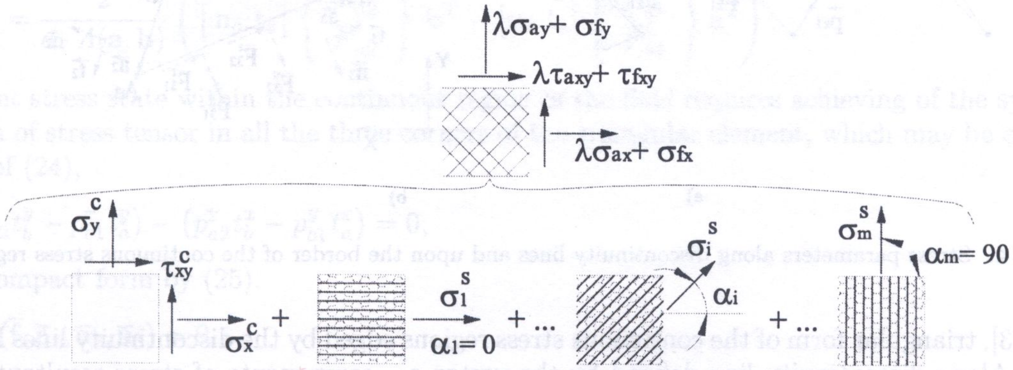

Fig. 3. Decomposition of total stresses upon the particular material stresses

If the stress vectors which proceed from active and volume load are defined with $\boldsymbol{\sigma}_a = \{\sigma_{ax}\ \sigma_{ay}\ \tau_{axy}\}^{\mathrm{T}}$, and $\boldsymbol{\sigma}_f = \{\sigma_{fx}\ \sigma_{fy}\ \tau_{fxy}\}^{\mathrm{T}}$ and stress vector in concrete and reinforcement as $\boldsymbol{\sigma}^{cs} = \{\sigma_x^c\ \sigma_y^c\ \tau_{xy}^c\ \sigma_1^s\ \sigma_2^s\ \Lambda\ \sigma_m^s\}^{\mathrm{T}}$, decomposition (15), in compact form, may be expressed in the form (16).

$$\Phi^{cs}\langle \lambda, \boldsymbol{\sigma}_a, \boldsymbol{\sigma}_f, \boldsymbol{\sigma}^{cs}\rangle = 0, \tag{16}$$

$$\Phi^{c}\left(\sigma_x^c, \sigma_y^c, \tau_{xy}^c\right) \leq 0, \tag{17}$$

$$\Phi_i^{s}\left(\sigma_i^s\right) \leq 0 \qquad i = 1, ..., m. \tag{18}$$

Following those definitions, concrete and reinforcement plasticity conditions (12) and (14) may be represented in the form (17) and (18).

$$\left\langle \begin{array}{c} \max \lambda \\ \Phi^{cs}\left\langle \lambda, \boldsymbol{\sigma}_a, \boldsymbol{\sigma}_f, \boldsymbol{\sigma}^{cs} \right\rangle = 0 \\ \Phi_c\left(\sigma_x^c, \sigma_y^c, \tau_{xy}^c\right) \leq 0 \\ \Phi_i^s\left(\sigma_i^s\right) \leq 0 \quad i = 1, ..., m \end{array} \right\rangle. \tag{19}$$

Finally, relations (16) to (18) represent plasticity condition of reinforced concrete (2), and the ultimate load task is defined by variational problem (19).

3. Stress field definition

The quality of approximation of the limit stress state in the reinforced concrete elements primarily depends on supposed stress distribution along discontinuity lines. The known solutions of simple discontinuous stress fields, as well as their construction are shown in [3]. Those solutions are based on the constant stress distribution along discontinuity lines. In some way, it reflects certain analogy with the truss models but, as it is shown in [9], stress fields construction is very limited and not suitable for application in the optimization methods of the field configuration. According to this reason, linear stress distribution along discontinuity lines and border sides with unknown stresses has been adopted.

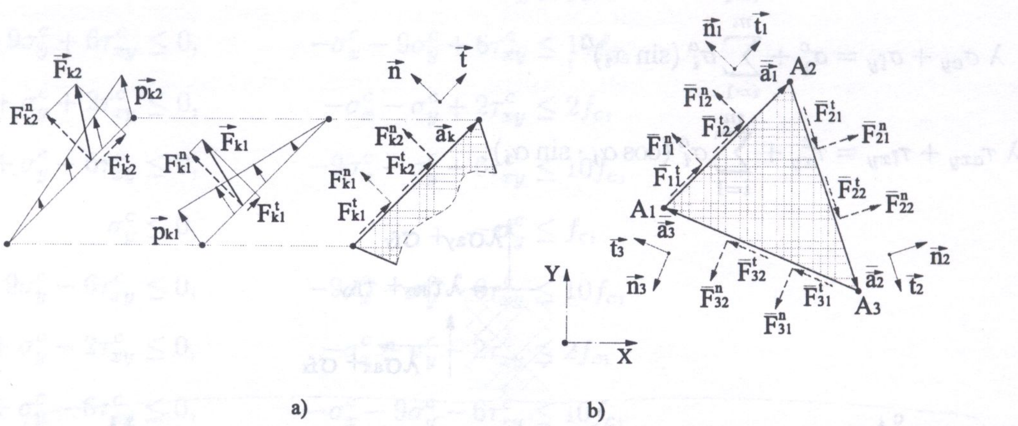

Fig. 4. Stress parameters along discontinuity lines and upon the border of the continuous stress region

As in [3], triangular form of the continuous stress regions edged by the discontinuity lines has been adopted. Along discontinuity line defined by the vector $\mathbf{a}_k$, components of stress resultants in the tangent and normal directions of a suitable discontinuity line have been adopted as stress parameters, figure 4a. Local orientation of continuous stress region border vectors, *stress field element sides* $\bar{\mathbf{a}}_1 - \bar{\mathbf{a}}_2 - \bar{\mathbf{a}}_3$, has been adopted to be clockwise. So, the stress state in continuous triangular stress region is defined by the stress resultant vector in the form (20).

$$\bar{\mathbf{f}} = \left\{ \left\{ \overline{F}^n_1 1\, \overline{F}^t_1 1\, \overline{F}^n_1 2\, \overline{F}^t_1 2 \right\} \left\{ \overline{F}^n_2 1\, \overline{F}^t_2 1\, \overline{F}^n_2 2\, \overline{F}^t_2 2 \right\} \left\{ \overline{F}^n_3 1\, \overline{F}^t_3 1\, \overline{F}^n_3 2\, \overline{F}^t_3 2 \right\} \right\}^T. \quad (20)$$

Consistent stress state within each triangular region of the field requires that components of the stress resultant vector $\bar{\mathbf{f}}$ satisfy the local equilibrium conditions (5) and (6), as well as global conditions (10) and (11).

In the corner, between the sides lengths' l_a and l_b, the stress state has been determined by the edge stress vectors along the borders $\mathbf{p}_a$ and $\mathbf{p}_b$, Fig. 5.

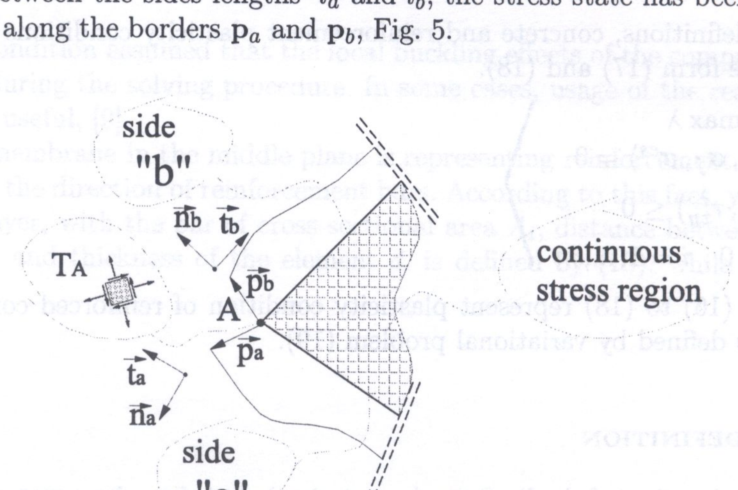

Fig. 5. Stress state in the corner of element

$$\mathbf{p}_{a2} = \left\{ \begin{array}{c} p_{a2}^{n} \\ p_{a2}^{t} \end{array} \right\} = \frac{2}{l_a} \left\{ \begin{array}{c} \overline{F}_{a2}^{n} \\ \overline{F}_{a2}^{t} \end{array} \right\}, \qquad \mathbf{p}_{b1} = \left\{ \begin{array}{c} p_{b1}^{n} \\ p_{b1}^{t} \end{array} \right\} = \frac{2}{l_b} \left\{ \begin{array}{c} \overline{F}_{b1}^{n} \\ \overline{F}_{b1}^{t} \end{array} \right\}. \tag{21}$$

For tangent and normal vectors of suitable border branches $\mathbf{n}_a$, $\mathbf{n}_b$, $\mathbf{t}_a$ and $\mathbf{t}_b$, and the designation,

$$\Lambda(\mathbf{a}, \mathbf{b}) = \mathbf{a}^{\mathrm{T}} \begin{bmatrix} 0 & 1 \\ -1 & 0 \end{bmatrix} \mathbf{b} \tag{22}$$

stress tensor in the corner is defined by (23).

$$\mathbf{T}_A = \frac{2}{d \cdot \Lambda(\mathbf{a}, \mathbf{b})} \left([\mathbf{n}_a\ \mathbf{t}_a] \left\{ \begin{array}{c} \overline{F}_{a2}^{n} \\ \overline{F}_{a2}^{t} \end{array} \right\} \mathbf{b}^{\mathrm{T}} - [\mathbf{n}_b\ \mathbf{t}_b] \left\{ \begin{array}{c} \overline{F}_{b1}^{n} \\ \overline{F}_{b1}^{t} \end{array} \right\} \mathbf{a}^{\mathrm{T}} \right). \tag{23}$$

Consistent stress state within the continuous region of the field requires achieving of the symmetry condition of stress tensor in all the three corners of the triangular element, which may be expressed in form of (24),

$$(p_{a2}^{x} t_b^{y} - p_{b1}^{x} t_a^{y}) - (p_{a2}^{y} t_b^{x} - p_{b1}^{y} t_a^{x}) = 0, \tag{24}$$

or in a compact form by (25).

$$\Sigma_A^T(\overline{\mathbf{f}}, \overline{\mathbf{a}}_1, \overline{\mathbf{a}}_2, \overline{\mathbf{a}}_3) = 0. \tag{25}$$

If all three conditions of the form (25) are satisfied, the global moment equilibrium condition is satisfied too (11). Apart from these conditions, the conditions of global force equilibrium (10) must also be satisfied, which, in the case of the presence of volume forces, may be expressed in form of (26).

$$\Sigma^X(\overline{\mathbf{f}}, \overline{\mathbf{a}}_1, \overline{\mathbf{a}}_2, \overline{\mathbf{a}}_3,\ f_x) = 0, \qquad \Sigma^Y(\overline{\mathbf{f}}, \overline{\mathbf{a}}_1, \overline{\mathbf{a}}_2, \overline{\mathbf{a}}_3,\ f_y) = 0. \tag{26}$$

The three conditions of the form (25) with the two conditions (26), consist the *conditions of existence of the continuous triangular region* in stress field in the case of adopted linear distribution of stress along discontinuity lines.

Bilinear stress state prevails inside continuous stress region, details of which are shown in [9]. Applying bilinear interpolation functions, the stress state in the point inside the region Q, which is determined by vector $\mathbf{x}_Q$ (Fig. 6),

$$\mathbf{x}_Q = \left\{ 1\ x_Q\ y_Q \right\}^{\mathrm{T}} \tag{27}$$

are defined according to the relation (28).

$$\mathbf{s}_Q = \left\{ \begin{array}{c} \sigma_Q^X \\ \sigma_Q^Y \\ \tau_Q^{XY} \end{array} \right\} = \begin{bmatrix} (\mathbf{x}_Q)^{\mathrm{T}}\ \mathbf{A}_X \\ (\mathbf{x}_Q)^{\mathrm{T}}\ \mathbf{A}_Y \\ (\mathbf{x}_Q)^{\mathrm{T}}\ \mathbf{A}_{XY} \end{bmatrix} \overline{\mathbf{f}}. \tag{28}$$

Matrices $\mathbf{A}_X$, $\mathbf{A}_Y$ and $\mathbf{A}_{XY}$ depend on geometry of triangular region, and their definitions are shown in detail in [9].

Strict satisfaction of the yield conditions, expressed by system (16)–(18), is achieved in three points inside the region Y_1, Y_2 and Y_3, according to the disposition in Fig. 6. Stress states at these points are defined by relation (28).

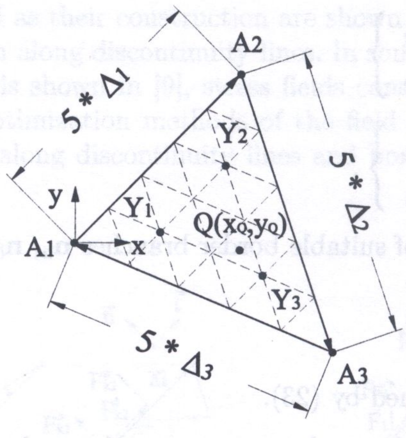

Fig. 6. Local coordinate system and yield check points disposition

4. Stress field optimization

The number of free parameters, which can be varied during optimization process, influences the possibility of optimization of discontinuous stress field. Apart from static edge sides, bound conditions may be set upon the bound parts according to displacements or in the mixed form, Fig. 7.

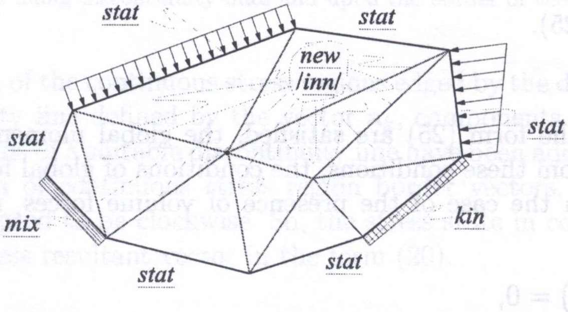

Fig. 7. Types of the discontinuous field bound sides

Homogenous kinematical bound conditions are treated by adequate unknown stress parameters of reactive stresses. For a field made up of n_{tr} of triangular continuous regions, number of sides of adequate type of the whole stress field will be designated with:

- n_{stat} – set of static bound conditions,
- n_{kin} – set of kinematics bound conditions,
- n_{mix} – set of mixed bound conditions,
- n_{new} – inner (new) sides, i.e. lines of discontinuity of stress field.

Number of unknown static parameters, which define discontinuous stress field including the outside load parameter $\lambda^{\mathrm{global}}$, is defined by (29).

$$n_{\mathrm{unkn}} \begin{pmatrix} n_{\mathrm{stat}} \\ n_{\mathrm{kin}} \\ n_{\mathrm{mix}} \\ n_{\mathrm{new}} \end{pmatrix} = 4 \cdot (n_{\mathrm{new}} + n_{\mathrm{kin}}) + 2 \cdot n_{\mathrm{mix}} + 1. \tag{29}$$

Consistency of the stress field requires satisfaction of three equations with the form (25) for each continuous region, as well as two equations of region global force equilibrium in the form (26), i.e. for the whole stress field is defined with equations (30).

$$n_{\mathrm{eq}} = 5 \cdot n_{\mathrm{tr}}. \tag{30}$$

The difference between the number of unknowns and the number of equations defines the number of static free parameters – *number of inside degrees of freedom of discontinuous stress field* n_{inn}, (31).

$$n_{\text{inn}} = 4 \cdot (n_{\text{kin}} + n_{\text{new}}) + 2 \cdot n_{\text{mix}} - 5 \cdot n_{\text{tr}} + 1. \tag{31}$$

Linearized yield conditions (19) must also be satisfied for each continuous region into the characteristic checkpoints Y_1, Y_2 and Y_3, according to the layout in Fig. 6. Optimization related to the inside degrees of freedom is defined by the linear programming (LP) problem (32)

$$\left\langle \begin{array}{c} \max \lambda \\ \Sigma^{X} \; (\overline{\mathrm{f}}^{l}, \overline{\mathrm{a}}_1^{l}, \overline{\mathrm{a}}_2^{l}, \overline{\mathrm{a}}_3^{l},) = 0 \\ \Sigma^{Y} \; (\overline{\mathrm{f}}^{l}, \overline{\mathrm{a}}_1^{l}, \overline{\mathrm{a}}_2^{l}, \overline{\mathrm{a}}_3^{l},) = 0 \\ \Sigma^{\tau}_{A_1} \; (\overline{\mathrm{f}}^{l}, \overline{\mathrm{a}}_1^{l}, \overline{\mathrm{a}}_2^{l}, \overline{\mathrm{a}}_3^{l},) = 0 \\ \Sigma^{\tau}_{A_2} \; (\overline{\mathrm{f}}^{l}, \overline{\mathrm{a}}_1^{l}, \overline{\mathrm{a}}_2^{l}, \overline{\mathrm{a}}_3^{l},) = 0 \\ \Sigma^{\tau}_{A_3} \; (\overline{\mathrm{f}}^{l}, \overline{\mathrm{a}}_1^{l}, \overline{\mathrm{a}}_2^{l}, \overline{\mathrm{a}}_3^{l},) = 0 \\ l=1, \; \Lambda, \; n_{\text{tr}} \end{array} \right\rangle \tag{32}$$

$$\left\langle \begin{array}{l} \Phi^{cs}_{jk} \, \langle \Lambda, \sigma_a, \sigma_f, \sigma^{cs} \rangle = 0 \\ \Phi^{c}_{jk} \, (\lambda, \sigma^c_x, \sigma^c_y, \tau^c_{xy}) \le 0 \\ \Phi^{s}_{ijk} \, (\sigma^s_j) \qquad i=1,\dots, m \\ \qquad j=1, \; \Lambda, \; n_{\text{tr}} \\ \qquad k=1, \; \Lambda, \; n_{\text{points}} \end{array} \right\rangle$$

with unknown variables:

- vectors of the stress resultants $\overline{\mathrm{f}}^{l}$ $l = 1, \Lambda, n_{\text{tr}}$ and
- concrete and reinforcement stress vectors $\{\sigma^c\}_{jk}$, $\{\sigma^s_i\}_{jk}$, $j = 1, \Lambda, n_{\text{tr}}$; $k = 1, \Lambda, n_{\text{points}}$.

A solution of such linear programming problem may be found out, beside the well known *Simplex algorithm*, by the more efficient so called *Interior-point methods*, which have been developed during the last decade. One of the most efficient and the most popular methods is the so-called *Mehrotra's predictor-corrector method*, whose implementation was developed by Vanderbei [16]. This *LOQO* package is available for research purposes, and is applied for solving large dimension LP program during this research.

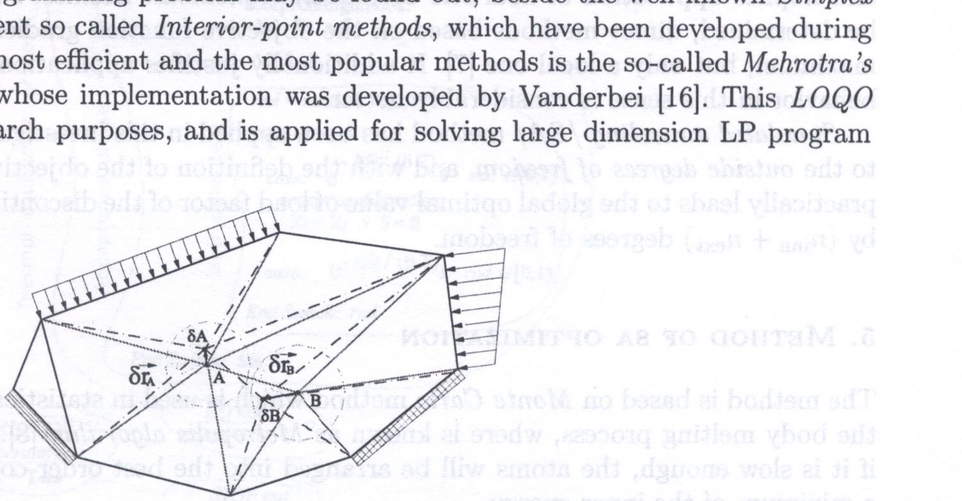

Fig. 8. Variation of the stress field configuration

Apart from the optimization related to the *inside degrees of freedom*, in static sense, this research takes into consideration the influence of the discontinuity line configuration on the quality of the *lower approximation of stress state* at the limit equilibrium of RC elements. Similar attempt is presented in the Sudermann's and Mutscher's paper [15], which presents the idea of the node positions optimization while applying *Strut-and-Tie* method of the load carrying capacity analysis.

The possibility of variation of discontinuous stress field configuration is conditioned by the initial configuration as well as by other factors such as reinforcement of RC elements, thickness and etc.

The number of parameters which determine configuration of discontinuous stress field is defined as the *number of outside /external/ degrees of freedom of discontinuous stress field*, with the designation n_{ext}. As distinguished from the number of *inside degrees of freedom* which is unambiguously determined by relation (31), *the number of outside degrees of freedom of stress field*, as mentioned, is conditioned by different factors and it should be determined in accordance with the present bounds of regions. Therefore, areas for variation of configuration parameters should be defined.

If coordinates of the discontinuity line node points are considerered as unknown, equations of global force equilibrium of elements in the X and Y direction (26), as well as equations of local moment equilibrium into the element's corners (25) become nonlinear, which leads us into the nonlinear programming (NP) area.

This problem may be solved by defining the objective function of the of nonlinear program related to n_{ext} *outside degrees of freedom* as an optimal solution of linear program related to n_{inn} *inside degrees of freedom.*

If we define vector of the configuration parameters, as

$$\delta\mathbf{X} = \left\{\delta X_1 \;\; \delta X_2 \;\; \Lambda \;\; \delta X_{n_{\text{ext}}}\right\}^{\mathrm{T}} \tag{33}$$

the load factor objective function may be expressed in the form (34).

$$\lambda_{\text{ext}}(\delta\mathbf{X}) = \lambda_{\text{inn}}^{\text{global}}\left(\delta\mathbf{X},\, \mathbf{f}^{\text{global}^*}\right) = \max_{\mathbf{f}_{\text{global}} \in R^{n_{\text{inn}}}} \left(\lambda_{\text{inn}}^{\text{global}}\left(\delta\mathbf{X}, \mathbf{f}^{\text{global}}\right) : R^{n_{\text{inn}}} \to R\right). \tag{34}$$

The separation of the optimization process results in considerable reduction of the dimension of nonlinear program. In spite of large dimension, the optimization problem related to the inside degrees of freedom, remain linear, and may be solved efficiently. During nonlinear optimization, very few informations of the objective function defined by (34) are known, i.e. only its value at actual point i.e. in the actual configuration of discontinuity lines. This fact makes application of direct methods in optimization process related to the outside degrees of freedom practically impossible, and implies application of heuristic *optimization methods.* Besides, since global maximum should be determined, direct methods based on the objective function gradients, cannot guarantee global maximum, but only a local one [7]. It additionally justifies application of heuristic methods whose behavior in this sense is considerably better.

Simulated annealing /SA/ method has been applied in this investigation for optimization related to the *outside degrees of freedom*, and with the definition of the objective function (34), the method practically leads to the global optimal value of load factor of the discontinuous stress field determined by $(n_{\text{inn}} + n_{\text{ext}})$ degrees of freedom.

5. Method of SA optimization

The method is based on *Monte Carlo* method which is used in statistical mechanics in simulation of the body melting process, where is known as *Metropolis algorithm* [8]. During the cooling process, if it is slow enough, the atoms will be arranged into the best order configuration, which results in a minimum of the inner energy.

Starting from very high temperature, by slow cooling process, thermal balance is established at every temperature, which is described by *Boltzmann distribution*,

$$\mathrm{P}\left(E = \tilde{E}\right) = \frac{e^{-\tilde{E}/(k_B\, T)}}{Z(T)} \tag{35}$$

of the probability that the system is in a state with the level of inner energy $\tilde{E}$. In expression (35), k_B is *Boltzmann's constant*, T is the present temperature, while the factor $e^{-\tilde{E}/k_B T}$ is so-called *Bolzmann's factor*. $Z(T)$ is the normalizing factor. While the temperature is falling, distribution (35) concentrates around the state with the lowest inner energy, until the temperature finally reaches zero value, where only the state with a minimum of inner energy has a probability different from zero.

Metropolis algorithm is used to establish thermal equilibrium at a particular temperature T, while new sequential states generate *Monte Carlo* method during simulation of annealing process.

Kirkpatrik et al. [4], have noticed a connection between the processes in statistical mechanics and the problem of combinatorial optimization expressed in necessity to establish a state with a minimum of energy i.e. a global minimum in the optimization process. The original idea of the application of *SA algorithm* to solve *NP-complete* discreet variables optimization problems [4], has been extended and applied to find optimal value of the continuous variable function in different areas of engineering, science and technology [12].

Specifications of the application of SA algorithm to the optimization continuous vector variable function, as the details of the algorithm adaptation to the problem of discontinuous stress fields configuration optimization are shown in [9]. Figure 9 presents an outline of the applied optimization

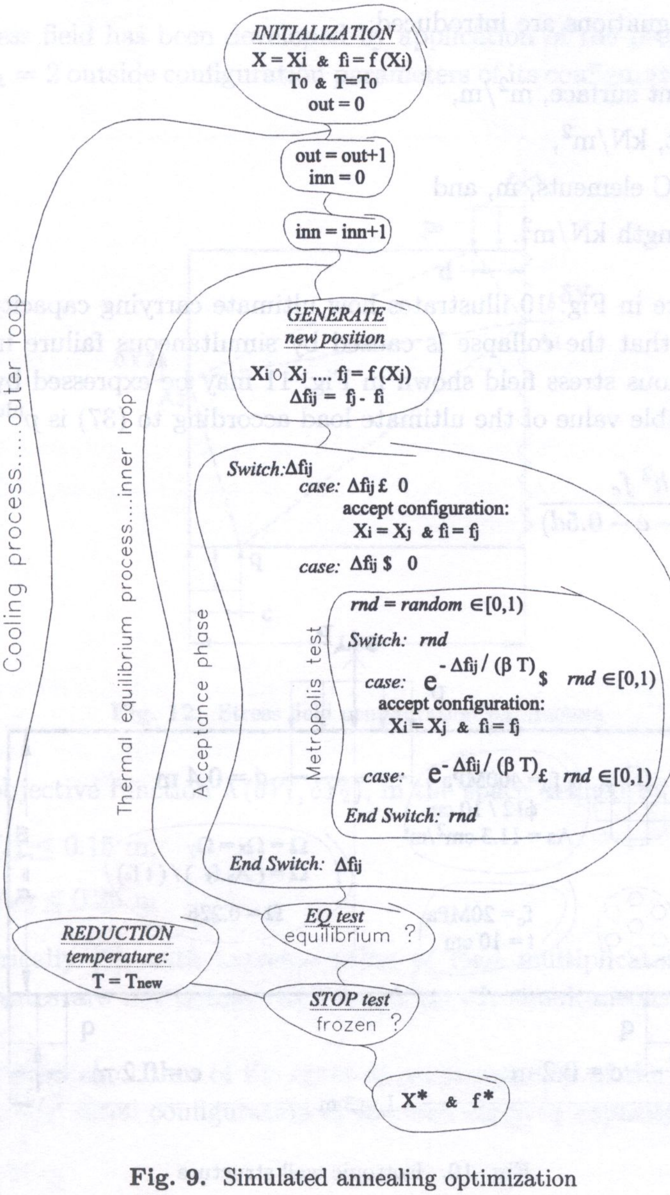

Fig. 9. Simulated annealing optimization

algorithm of real function of vector variable $f(\mathbf{X})$. Details of each phase, initiation, generation of a new configuration, checking of thermal equilibrium establishment, temperature reduction and stopping criterion are shown in detail in [9]. It should be pointed out that the so-called homogenous type of *SA* algorithm has been implemented.

6. Applications in determining ultimate carrying capacity

The discontinuous stress fields' optimization procedure has been implemented in the program package *D & OSF – Developer & Optimizer of the Stress Fields,* developed under *METLAB for Windows* surrounding. This package manages determination load carrying capacity of RC elements in plane stress state.

The presence of reinforcement is defined by the ratio of limit stresses in tension and pressure, by reinforcement degree Ω in the form

$$\Omega = \frac{A_s\, f_y}{t\, f_c} \tag{36}$$

where the following designations are introduced:

- A_s .... reinforcement surface, m^2/m,
- f_y ... yielding limit, kN/m^2,
- t.... thickness of RC elements, m, and
- f_c ... concrete strength kN/m^2.

Example of the structure in Fig. 10 illustrates how ultimate carrying capacity is determined. Following the assumption that the collapse is caused by simultaneous failure in the symmetry axis cross-section, discontinuous stress field shown in Fig. 11 may be expressed by that failure mechanism, Nielsen [11]. Suitable value of the ultimate load according to (37) is $p^{\mathrm{ult}} = 0.709$ MN/m.

$$p^{\mathrm{ult}} = \frac{2\,\Omega\, t,\, h^2\, f_c}{(1+\Omega)\,(L-c-0.5d)}\,. \tag{37}$$

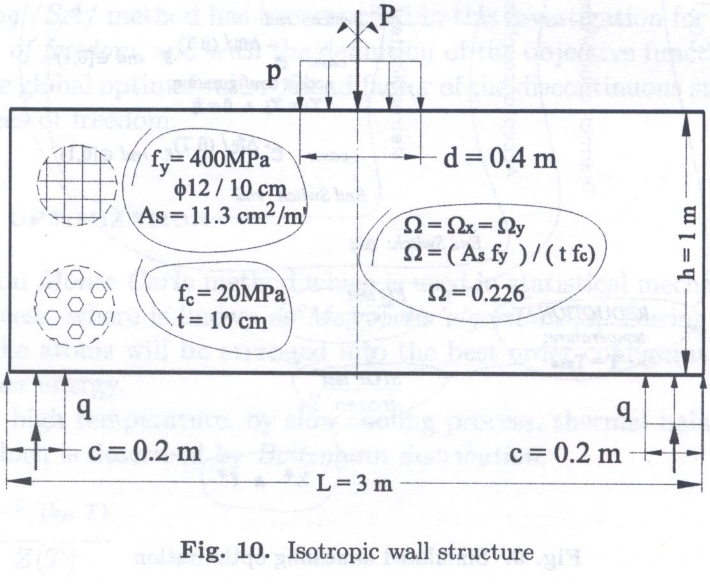

Fig. 10. Isotropic wall structure

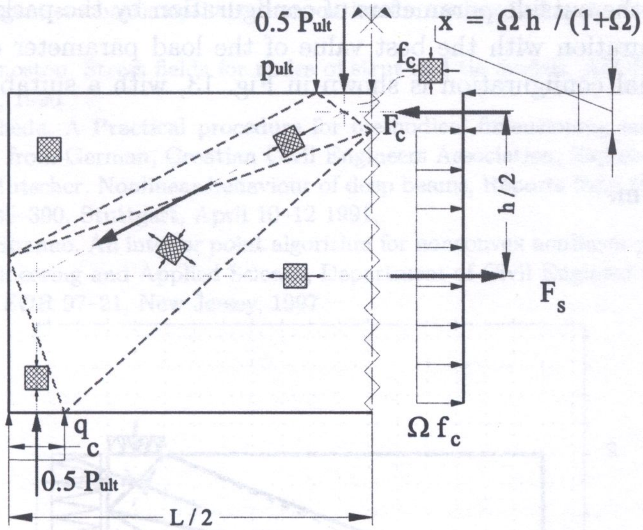

Fig. 11. Stress field in the limit equilibrium

Discontinuous stress field has been developed by application of the program package *D & OSF*, with the adopted $n_{\text{ext}} = 2$ outside configuration parameters of its configuration and $p_0 = 1.0$ MN/m, Fig. 12.

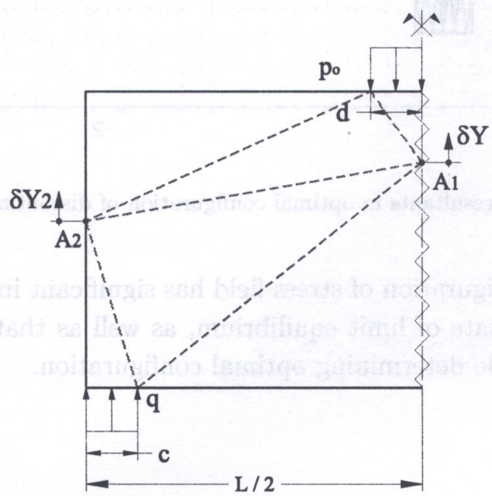

Fig. 12. Stress field configuration parameters

Load parameter objective function $\lambda\left(\delta Y_1, \delta Y_2\right)$, in the space defined by (38),

$$-0.15\ \text{m} \leq \delta Y_{A1} \leq 0.15\ \text{m},$$
$$-0.25\ \text{m} \leq \delta Y_{A2} \leq 0.25\ \text{m} \qquad (38)$$

is determined numerically [9], with extreme value of load multiplicator $\lambda^{\text{opt}} = 0.706$, at the point where its derivates are not defined and which match simultaneous failure in concrete and reinforcement.

Presented optimization algorithm of the inner stress parameters of the stress field is found out, initial value, matches the initial configuration of the load carrying capacity given by (39).

$$p^{0*}_{\text{opt}} = 0.537\ \text{MN/m}. \qquad (39)$$

During optimization of the outside parameters of configuration by the package *D & OSF* limit load value in optimal configuration with the best value of the load parameter of $\lambda^* = 0.705$ has been determined. This optimal configuration is shown in Fig. 13, with a suitable ultimate load (40) is determined.

$$p^*_{\text{opt}} = 0.705 \text{ MN/m}. \tag{40}$$

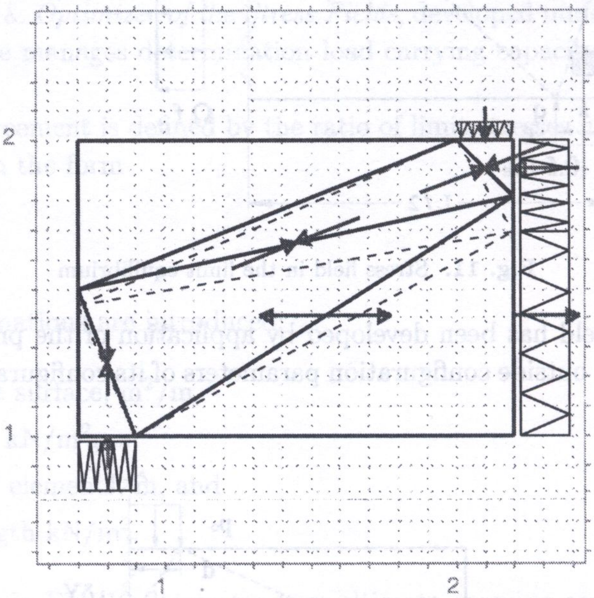

Fig. 13. Stress resultants in optimal configuration of discontinuous stress field

It may be concluded that configuration of stress field has significant influence on the approximation of stress distribution in the state of limit equilibrium, as well as that applied *simulated annealing* algorithm is very efficient while determining optimal configuration.

References

[1] M. Aćić. A contribution to solving the problem of the limit states of reinforced concrete wall structures, Ph.D. thesis. The Faculty of Civil Engineering of the University of Belgrade, Belgrade, 1978.

[2] G. Dahlquist, A. Bjork. Numerical methods. Prentice-Hall, Englewood Cliffs, New Jersey, 1974.

[3] R. Hajdin. Computerunterstutzte Berechnung von Stahlbetonscheiben mit Spannungsfeldern, Dissertation, Institute of Structural Engineering, ETH Zurich, Zurich, 1990.

[4] S. G. Kirkpatrick, Jr. Gelatt. M. P. Vecchi. Optimization by simulated annealing. *Science*, **220** (4598): 671–680, 1983.

[5] M. D. Kostovos, M. N. Pavlović. Structural concrete. *Thomas Telford Publications*, London, 1995.

[6] P. Marti. Basic tools of reinforced concrete beam design, *Journal of ACI*, **82** (1): 46–56, 1985.

[7] G. P. Mc Cormick. Nonlinear Programming: Theory, Algorithms and Applications, John Wiley, New York, 1980.

[8] N. Metropolis, A. Rosenbluth, A. Teller, E. Teller. Equations of state calculations by fast computing machines, *Journal of Chemical Physics*, **21** (5): 1087–1092, 1953.

[9] Z. Mišković. Application of stress fields based on the theory of plasticity for determination load carrying capacity of reinforced concrete wall, Ph.D. Theses. The Faculty of Civil Engineering, University of Belgrade, 2000.

[10] P. Muller. Plastische Berechnung von Stahlbetonscheiben und–balken, Bericht Nr. 83. Institut fur Baustatik und Konstruktion, ETH Zurich, 1985.

[11] M. P. Nielsen. Limit Analysis and concrete plasticity. Prentice-Hall, Inc., Englewood cliffs, New Jersey, 1984.

[12] G. T. Parks. An intelligent stochastic optimization routine for nuclear fuel cycle design. *Nuclear Technology*, **89**: 233–246, 1990.

[13] M. Schlaich, G. Anagnostou. Stress fields for nodes of strut-and-tie models, ASCE *Journal of Structural Engineering*, **116** 1: 13–22, 1990.

[14] J. Schlaich, D. Weischede. A Practical procedure for methodical fimensioning and construction in reinforced concrete – translation from German, Croatian Civil Engineers Association, Zagreb, 1987.

[15] W. Sundermann, P. Mutscher. Nonlinear behaviour of deep beams, Reports from the IABSE Colloquium Structural Concrete, **62**: 385–390, Stuttgart, April 10–12 1991,

[16] R. J. Vanderbei, D. F.Shanno. An interior point algorithm for nonconvex nonlinear programming, Princeton University, School of Engineering and Applied Science, Department of Civil Engineering and Operations Research, Technical Report No. SOR 97–21, New Jersey, 1997.